

# Journal of Materials Chemistry A

Accepted Manuscript



This is an *Accepted Manuscript*, which has been through the Royal Society of Chemistry peer review process and has been accepted for publication.

*Accepted Manuscripts* are published online shortly after acceptance, before technical editing, formatting and proof reading. Using this free service, authors can make their results available to the community, in citable form, before we publish the edited article. We will replace this *Accepted Manuscript* with the edited and formatted *Advance Article* as soon as it is available.

You can find more information about *Accepted Manuscripts* in the [Information for Authors](#).

Please note that technical editing may introduce minor changes to the text and/or graphics, which may alter content. The journal's standard [Terms & Conditions](#) and the [Ethical guidelines](#) still apply. In no event shall the Royal Society of Chemistry be held responsible for any errors or omissions in this *Accepted Manuscript* or any consequences arising from the use of any information it contains.

Cite this: DOI: 10.1039/c0xx00000x

www.rsc.org/xxxxxx

## COMMUNICATION

# Co<sub>3</sub>O<sub>4</sub> microcubes with exceptionally high conductivity using CoAl layered double hydroxide precursor via soft chemically synthesized cobalt carbonate

Churchil A. Antonyraj,<sup>a</sup> Divesh N. Srivastava,<sup>b</sup> Gurudas P. Mane,<sup>c</sup> Sivashunmugam Sankaranarayanan,<sup>a</sup> Ajayan Vinu,<sup>c,d</sup> and Kannan Srinivasan<sup>a\*</sup>

Received (in XXX, XXX) Xth XXXXXXXXXX 20XX, Accepted Xth XXXXXXXXXX 20XX

DOI: 10.1039/b000000x

Cubic micro particles of Co<sub>3</sub>O<sub>4</sub> spinel were synthesized by calcination of CoCO<sub>3</sub> obtained using CoAl layered double hydroxide (LDH) as a unitary precursor through soft-chemical decomposition. The obtained cobalt spinel showed an exceptionally high electrical conductivity at room temperature. This is attributed to high concentrations of charge carriers (Co<sup>4+</sup>), unique morphology, high reduction temperature and low activation barrier.

Co<sub>3</sub>O<sub>4</sub> spinel is a well-studied material with diverse applications such as energy storage and conversion, and catalysis.<sup>1-3</sup> It is potentially explored as a negative electrode in rechargeable lithium batteries.<sup>4</sup> One of the challenges addressed recently is to enhance the electronic conductivity of Co<sub>3</sub>O<sub>4</sub>, which is generally achieved by partially substituting cobalt ions with other metal ions such as Li, Al, Ga, Ge, and Sn besides transition metal ions such as Ni.<sup>5,6</sup> Among them, substitution of Li offers a significant increase in the conductivity with respect to neat Co<sub>3</sub>O<sub>4</sub>.<sup>7</sup> This was attributed to the presence of Co<sup>4+</sup> (for charge compensation of Li<sup>+</sup>), thus allowing delocalization of holes in the octahedral sites of the spinel lattice and thereby enhancing the conductivity.<sup>8</sup> An approach has also been made to synthesize nanostructured composites of Co<sub>3</sub>O<sub>4</sub> with C, Al<sub>2</sub>O<sub>3</sub> etc. to improve conductivity.<sup>9</sup> Morphology of Co<sub>3</sub>O<sub>4</sub> plays an important role in controlling the electronic properties, which in turn is governed by the nature of precursors.<sup>2</sup> Being a rarely studied precursor for the synthesis of Co<sub>3</sub>O<sub>4</sub>, morphology of cobalt carbonate (CoCO<sub>3</sub>) is known to influence the final property of the spinel.<sup>10</sup> Recently, Co<sub>3</sub>O<sub>4</sub> spinel derived from CoCO<sub>3</sub> showed superior gas sensing properties.<sup>11</sup> It is thus always inquisitive to find a novel synthetic strategy for Co<sub>3</sub>O<sub>4</sub> with improved electronic properties using different precursors with tunable morphology.

Layered double hydroxides (LDHs) are ionic lamellar compounds consist of positively charged hydroxide sheets with interlayers filled with anions and water molecules. LDHs are widely used as catalysts, catalyst supports, composites, coatings and thin films for diverse applications.<sup>12-16</sup> During our investigation on the synthesis of CoAl-LDH by different methodologies, urea hydrolysis resulted in the formation of phase pure LDH; hydrothermal treatment in mother liquor turned this LDH into cobalt carbonate (denoted here as CoCO<sub>3</sub>-L).<sup>‡</sup>

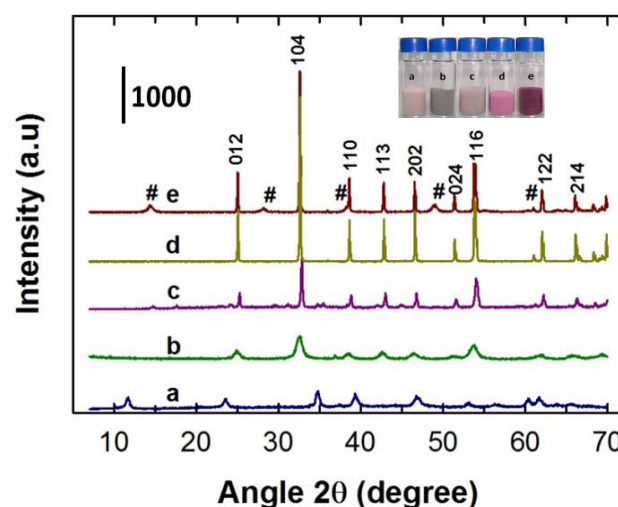


Fig.1 PXRD of (a) CoAl-LDH, (b) CoCO<sub>3</sub>-C, (c) CoCO<sub>3</sub>-P, (d) CoCO<sub>3</sub>-U, (e) CoCO<sub>3</sub>-L, # Aluminium oxyhydroxide (AlOOH), (Inset is photograph of synthesized materials)

Heating thus produced carbonate in air topotactically converted it to Co<sub>3</sub>O<sub>4</sub> spinel with unique microcubic morphology and unusually high electrical conductivity at room temperature. Furthermore, the electrical conductivity observed is the highest considering unmodified Co<sub>3</sub>O<sub>4</sub> reported in literature and the reasons behind thereof are discussed. For comparison, cobalt carbonate was also synthesized by direct urea hydrolysis of Co(NO<sub>3</sub>)<sub>2</sub> and co-precipitation which are labelled as CoCO<sub>3</sub>-U and CoCO<sub>3</sub>-P, respectively. A commercial cobalt carbonate was also used, denoted as CoCO<sub>3</sub>-C (Experimental Section†). Powder X-ray diffraction pattern (PXRD) showed LDH phase for the urea hydrolysed sample (Fig. 1, a; JCPDS: 41-1428) and spherocobaltite phase (CoCO<sub>3</sub>; Fig. 1, e; JCPDS: 11-0692 whose reflections are indexed) for the sample after hydrothermal treatment. Less intense reflections of cobalt carbonate phase were observed for CoCO<sub>3</sub>-P (crystallite size - 378 Å) and CoCO<sub>3</sub>-C (crystallite size - 93 Å) than that of CoCO<sub>3</sub>-U (crystallite size - 550 Å) and CoCO<sub>3</sub>-L (crystallite size - 472 Å), suggest the influence of synthesis method in controlling the crystallinity of the samples. Conversion of LDH into carbonate critically depended on the hydrothermal treatment temperature wherein the

transformation is complete only above 150 °C (Fig. S1†). CoCO<sub>3</sub>-L from LDH had AlOOH as additional poorly crystalline phase (from Al present in the precursor CoAl-LDH; JCPDS: 21-1307). To remove this phase, it was treated with dilute HCl (3.3 mM). It is reported earlier that this concentration does not affect the LDH structure.<sup>17</sup> PXRD revealed that the structure of CoCO<sub>3</sub> was intact and confirmed the absence of aluminium oxide phase after the acid treatment (Fig. S2†). However, SEM-EDAX analysis of the acid-treated sample (Fig. S3†) showed the presence of aluminium and cobalt infers the presence of X-ray amorphous aluminium phase in the material that was not removed by acid treatment. Strategically, after acid treatment, the material was washed with water until neutral pH and then treated with various concentrations of NaOH (1 M, 50 mM and 5 mM). 5 mM of NaOH was sufficient to remove the aluminium completely. Simple base treatment alone was not sufficient to completely remove the AlOOH species. Further, treating washed and dried sample after pH adjustment under similar hydrothermal treatment did not yield carbonate phase, instead gave highly crystalline LDH phase. The schematic presentation of experiments conducted is given in electronic supplementary Information†. CoAl-LDH showed platelet-like morphology (Fig. S4a,† 3-5 μm) aggregated to flower like structure; CoCO<sub>3</sub>-L showed the layered structure assembled cubic morphology (Fig. S4b,† 30-50 μm) which is completely different from other reported morphologies of cobalt carbonate.<sup>18,19</sup> Formation of such layered cubic structure is probably due to the sheet-like morphology of the precursor LDH. In order to discern the reaction mechanism, hydrothermal treatment of freshly synthesized CoAl-LDH in mother liquor was carried out at different time and the phase formation, morphology, concentration of metal ions and pH was monitored (Fig. S5,†). Formation of CoCO<sub>3</sub> preceded initially by the partial transformation of carbonate-LDH to nitrate-LDH in 2 h. At 4 h, transformation of LDH to CoCO<sub>3</sub> occurred where the pH was higher (9.0) which showed rectangular to hexagonal nano flakes that assembled to form micro sheets which overlaid one over the other forming microcubes. Based on these studies, the reaction chemistry involved and a schematic mechanism are proposed and given in Fig. S5,†. Thermal stability of cobalt carbonates varied significantly with the synthetic procedure employed. CoCO<sub>3</sub>-C showed poor stability, decomposing completely at 349 °C while CoCO<sub>3</sub>-L was highly thermally stable (complete decomposition at 507 °C), the highest reported in literature so far (Fig. S6†).<sup>20,11</sup> A weight loss of 32.9% was observed at 430 °C ascribed to the conversion of CoCO<sub>3</sub>-L to Co<sub>3</sub>O<sub>4</sub>-L and is similar to the theoretically calculated value of 32.5%. Different cobalt carbonate samples were calcined in air at 500 °C for 3 h which showed the formation of Co<sub>3</sub>O<sub>4</sub> spinel as elucidated by PXRD (Fig. 2; JCPDS:42-1467). SEM analysis of these spinels showed varied morphology (Fig. 3) depending on the synthesis methodology employed. The unique layered structure assembled cubic morphology was retained for Co<sub>3</sub>O<sub>4</sub>-L although with significant roughness (craters are clearly visible on the surface of these particles; Fig. 3d inset). Co<sub>3</sub>O<sub>4</sub>-U showed a cubic morphology made up of highly crystalline small cubes as reported earlier.<sup>21</sup> On the other hand, Co<sub>3</sub>O<sub>4</sub>-P exhibited uniform cuboidal structure piled up together to form micro spheres of irregular shape whereas Co<sub>3</sub>O<sub>4</sub>-C displayed a small dumbbell

shaped morphology. The samples showed surface roughness probably due to the formation of pores created by the CO<sub>2</sub> evolution during calcination.

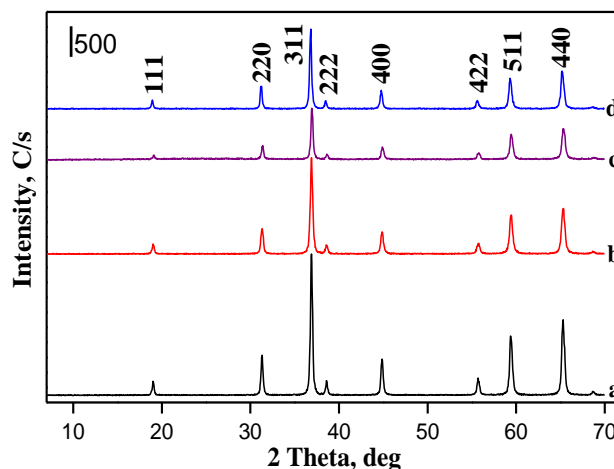


Fig. 2 PXRD patterns of (a) Co<sub>3</sub>O<sub>4</sub>-C, (b) Co<sub>3</sub>O<sub>4</sub>-P, (c) Co<sub>3</sub>O<sub>4</sub>-U, (d) Co<sub>3</sub>O<sub>4</sub>-L

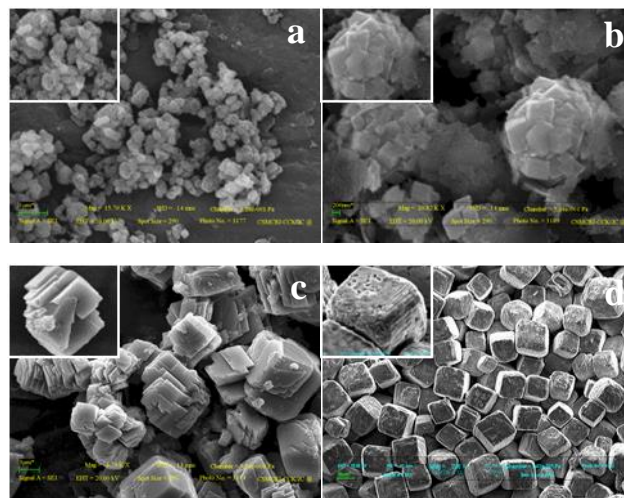


Fig. 3 SEM images of (a) Co<sub>3</sub>O<sub>4</sub>-C, (b) Co<sub>3</sub>O<sub>4</sub>-P, (c) Co<sub>3</sub>O<sub>4</sub>-U, (d) Co<sub>3</sub>O<sub>4</sub>-L (inset: HRSEM images)

Crystallite sizes of these morphologically different spinels are 265, 224, 255 and 253 Å and surface areas are 23, 25, 15, and 16 m<sup>2</sup>g<sup>-1</sup> for Co<sub>3</sub>O<sub>4</sub>-C, Co<sub>3</sub>O<sub>4</sub>-P, Co<sub>3</sub>O<sub>4</sub>-U and Co<sub>3</sub>O<sub>4</sub>-L respectively. Temperature programmed reduction (TPR) profiles of different Co<sub>3</sub>O<sub>4</sub> displayed two reduction peaks; the first reduction peak around 240 to 310 °C corresponds to the reduction of Co<sub>3</sub>O<sub>4</sub> to CoO, while the subsequent reduction of CoO to Co is observed at 310 to 410 °C (Fig. S7†). The reduction temperatures strongly depended on the morphology wherein Co<sub>3</sub>O<sub>4</sub>-L showed the highest reduction temperature.<sup>22</sup> Researchers have demonstrated the importance of morphologically different Co<sub>3</sub>O<sub>4</sub> materials for various electrochemical applications.<sup>1,20,23</sup> The current-voltage (I-V) characteristics of these materials were recorded in ±10 voltage window (Fig. 4), using automatic sweep mode. The slopes of the I-Vs were found to be linear (R<sup>2</sup> = 0.99 or better) in the scanned voltage range indicate ohmic nature of the contacts and the

existence of a single charge carrier.  $\text{Co}_3\text{O}_4$  is a p-type semiconductor with holes as charge carriers, primarily by  $\text{Co}^{4+}$  ions generated through several pathways namely charge disproportionation, partial substitution of cobalt in tetrahedral sites by monovalent ions such as  $\text{Li}^+$  and due to excess oxygen non-stoichiometry.<sup>24,25</sup> From the slopes of the I-V curves, the conductivity of the  $\text{Co}_3\text{O}_4$ -L is 1 to 5 order of magnitude higher ( $8.27 \times 10^{-4}$  S/cm) than that of the other  $\text{Co}_3\text{O}_4$  materials ( $1.14 \times 10^{-5}$  S/cm,  $6.73 \times 10^{-9}$  S/cm and  $4.48 \times 10^{-8}$  S/cm for  $\text{Co}_3\text{O}_4$ -U,  $\text{Co}_3\text{O}_4$ -P and  $\text{Co}_3\text{O}_4$ -C respectively).

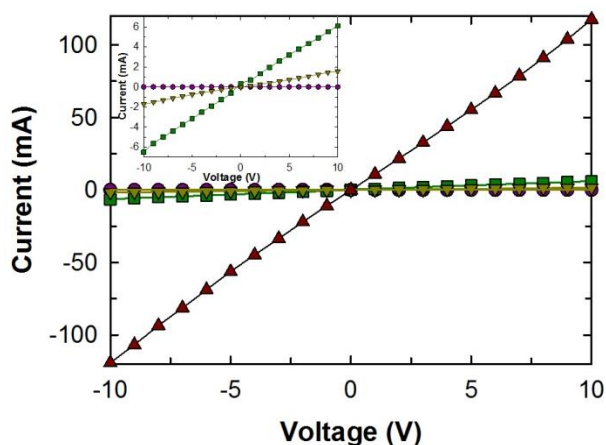


Fig. 4 RT Current-Voltage graphs of (●)  $\text{Co}_3\text{O}_4$ -P, (▼)  $\text{Co}_3\text{O}_4$ -C, (■)  $\text{Co}_3\text{O}_4$ -U, (▲)  $\text{Co}_3\text{O}_4$ -L (Inset: expanded region for first three samples)

This value is significantly higher than the classical  $\text{Co}_3\text{O}_4$  and compares well with the alkali incorporated  $\text{Co}_3\text{O}_4$  obtained through electrooxidation of  $\text{CoO}$ .<sup>25</sup> The possibility of contribution from Al in the improved conductivity of  $\text{Co}_3\text{O}_4$ -L was ruled out from elemental analysis measurements (<2 wt.%). The electrical conductance of cobalt oxide materials are best explained by “small-polaron model”, that involves the transport of localized charge states (holes as charge carriers).<sup>26</sup> Unusual high conductance for this sample is probably due to higher concentration of charge carriers (here  $\text{Co}^{4+}$ ) and unique layered cubic morphology that imparts better p-type electrical conductivity. This was supported through iodometric titration measurements that showed higher value of  $\text{Co}^{4+}$  (Table 1S†). It is worth noting here that the higher reduction temperature exhibited by  $\text{Co}_3\text{O}_4$ -L (Fig. S7†) supports facile formation of  $\text{Co}^{4+}$  by oxidation of  $\text{Co}^{3+}$ . Further, the conductivity of  $\text{Co}_3\text{O}_4$  increased with an increase in calcination temperature for  $\text{CoCO}_3$ -L (Table 2S†).<sup>25</sup> The conductance recorded as a function of temperature showed an increase with an increase in temperature that confirms the semiconducting nature. The energy of activation calculated from the slope of  $\ln(\rho/T)$  vs.  $1/T$  plot (Fig. S8†) was 0.50 eV, 0.70 eV, 0.58 eV and 0.17 eV for  $\text{Co}_3\text{O}_4$ -C,  $\text{Co}_3\text{O}_4$ -P,  $\text{Co}_3\text{O}_4$ -U and  $\text{Co}_3\text{O}_4$ -L respectively. The low activation energy observed for  $\text{Co}_3\text{O}_4$ -L correlates well with the enhanced conductivity of this sample.<sup>25</sup>

## Conclusions

In conclusion, we have successfully demonstrated the synthesis of crystalline cubic micro particles of  $\text{Co}_3\text{O}_4$  using  $\text{CoAl}$ -LDH as the unitary precursor via  $\text{CoCO}_3$  for the first time. Exceptionally

high electrical conductivity at room temperature was noted for this spinel and is attributed to higher charge carriers, unique morphology, low band gap, and higher reduction temperature. Such unusual properties possessed by this sample even without additional doping may find application as electrodes in batteries or supercapacitors with improved practical efficiency.

## Acknowledgements

The authors thank reviewers for their constructive suggestions that have helped in improving the scientific quality of the manuscript. The authors thank Council of Scientific and Industrial Research (CSIR), New Delhi for funding this work. C. A. A. thanks CSIR, New Delhi for the award of a Senior Research Fellowship (31/28(95)/2008-EMR-1.

## Notes and references

- <sup>a</sup> Discipline of Inorganic Materials & Catalysis, Central Salt and Marine Chemicals Research Institute, Council of Scientific and Industrial Research (CSIR), GB Marg, Bhavnagar 364002, India, \* Tel: +91-278-2567760 ext. 7030. Fax: +91-278-2567562. E-mail: skannan@csmcri.org; kanhem1@yahoo.com;
- <sup>b</sup> Analytical Discipline and Centralized Instrument Facility, Central Salt and Marine Chemicals Research Institute, Council of Scientific and Industrial Research (CSIR), GB Marg, Bhavnagar 364002, India
- <sup>c</sup> International Center for Materials Nanoarchitectonics, World Premier International Research Center, National Institute for Materials Science, 1-1 Namiki, Tsukuba, Ibaraki 305-0044, Japan
- <sup>d</sup> Multifunctional Nanoporous Materials Group, Australian Institute for Bioengineering and Nanotechnology (AIBN), The University of Queensland, Corner College and Cooper Roads, Brisbane Qld 4072, Australia

† Electronic Supplementary Information (ESI) available: [Synthetic procedures, reaction chemistry, mechanistic studies, PXRD, FT-IR, SEM-EDAX, HRSEM, DTGA, TPR, elemental analysis, oxygen content analysis and electrical conductivity measurements of various materials.]. See DOI: 10.1039/b000000x/

‡ Hydrothermal treatment of thoroughly washed urea-hydrolysed sample (and not in mother liquor) did not result in the formation of cobalt carbonate, but yielded a highly crystalline LDH. This provides evidence that the pH of the solution during hydrothermal treatment is critical for obtaining carbonate.

- B. Guo, C. Li, and Z. Yuan, *J. Phys. Chem. C*, 2010, **114**, 12805.
- T. Zhu, J. S. Chen and X. W. Lou, *J. Mater. Chem.*, 2010, **20**, 7015.
- X. Xie, Y. Li, Z. Liu, M. Haruta and W. Shen, *Nature*, 2009, **458**, 746.
- B. C. Yu, J. O. Lee, J. H. Song, C. M. Park, C. K. Lee and H. J. Sohn, *J. Solid State Electrochem.*, 2012, **16**, 2631.
- D. Pyke, K. K. Mallick, R. Reynolds and A. K. Bhattacharya, *J. Mater. Chem.*, 1998, **8**, 1095.
- J. A. K. Tareen, A. Malecki, J. P. Doumerc, J. C. Launay, P. Dordor, M. Pouchard and P. Hagenmuller, *Mater. Res. Bull.*, 1984, **19**, 989.
- E. Antolini, *Mater. Res. Bull.*, 1997, **32**, 9.
- E. Zhecheva, R. Stoyanova and S. Angelov, *Mater. Chem. Phys.*, 1990, **25**, 351.
- Y. Wang, H. J. Zhang, L. Lu, L. P. Stubbs, C. C. Wong and J. Lin, *ACS Nano*, 2010, **4**, 4753.
- H-P. Cong and S-H. Yu, *Cryst. Growth Des.*, 2009, **9**, 210.
- C. C. Li, X. M. Yin, T. H. Wang and H. C. Zeng, *Chem. Mater.*, 2009, **21**, 4984.
- C. A. Antonyraj, M. Gandhi and S. Kannan, *Ind. Eng. Chem. Res.*, 2010, **49**, 6020.
- T. Mitsudome, A. Noujima, Y. Mikami, T. Mizugaki, K. Jitsukawa and K. Kaneda, *Angew. Chem. Int. Ed.*, 2010, **49**, 5545.
- C. A. Antonyraj, P. Koilraj and S. Kannan, *Chem. Commun.*, 2010, **46**, 1902

- 
- 15 J. Han, Y. Dou, M. Wei, D. G. Evans and X. Duan, *Angew. Chem. Int. Ed.*, 2010, **49**, 2171.
- 16 X. Guo, F. Zhang, D. G. Evans and X. Duan, *Chem. Commun.*, 2010, **46**, 5197.
- 5 17 N. Iyi, T. Matsumoto, Y. Kaneko and K. Kitamura, *Chem. Mater.*, 2004, **16**, 2926.
- 18 D. S. Wang, T. Xie, Q. Peng, S. Y. Zhang, J. Chen and Y. D. Li, *Chem. Eur. J.*, 2008, **14**, 2507.
- 19 L. Hu, Q. Peng and Y. Li, *J. Am. Chem. Soc.*, 2008, **130**, 16136.
- 10 20 M. Y. Nassar and I. S. Ahmed, *Polyhedron*, 2011, **30**, 2431.
- 21 J. Feng and H. C. Zeng, *Chem. Mater.*, 2003, **15**, 2829.
- 22 X. Xie and W. Shen, *Nanoscale*, 2009, **1**, 50.
- 23 H. Nguyen and S. A. El-Safty, *J. Phys. Chem. C*, 2011, **115**, 8466.
- 24 P. H. T. Ngamou and N. Bahlawane, *Chem. Mater.*, 2010, **22**, 4158.
- 15 25 M. Douin, L. Guerlou-Demourgues, M. Menetrier, E. Bekaert, L. Goubault, P. Bernard and C. Delmas, *Chem. Mater.*, 2008, **20**, 6880.
- 26 C. F. Windisch, K. F. Ferris, G. J. Exarhos and S. K. Sharma, *Thin Solid Films*, 2002, **420**, 89.